

1 **Unexpected Death of a Duchenne Muscular Dystrophy Patient in an N-of-1 Trial of rAAV9-**  
2 **delivered CRISPR-transactivator**

3  
4 Angela Lek<sup>1,2\*</sup> Ph.D., Brenda Wong<sup>3\*</sup> M.D., Allison Keeler<sup>3,5</sup> Ph.D., Meghan Blackwood<sup>5</sup>, Kaiyue  
5 Ma<sup>1</sup>, Shushu Huang<sup>1</sup> M.D., Katelyn Sylvia<sup>5</sup>, Ana Rita Batista<sup>4,5</sup> Ph.D., Rebecca Artinian<sup>3,5</sup>,  
6 Danielle Kokoski<sup>3,5</sup>, Shestruma Parajuli<sup>5</sup>, Juan Putra<sup>6</sup> M.D., Chrystalle Katte Carreon<sup>6</sup> M.D., Hart  
7 Lidov<sup>6</sup> M.D. Ph.D., Keryn Woodman<sup>1</sup> Ph.D., Sander Pajusalu<sup>1,7,8</sup> M.D. Ph.D., Janelle M.  
8 Spinazzola<sup>9</sup> Ph.D., Thomas Gallagher<sup>5</sup> Ph.D., Joan LaRovere<sup>10</sup> M.D., Diane Baulderson<sup>11</sup> Ph.D.,  
9 Lauren Black<sup>12</sup> Ph.D., Keith Sutton<sup>12</sup> Ph.D., Richard Horgan<sup>13</sup>, Monkol Lek<sup>1\*</sup> Ph.D., Terence  
10 Flotte<sup>3,5\*</sup> M.D.

- 11  
12 1. Department of Genetics, Yale School of Medicine, New Haven, CT, USA.  
13 2. Muscular Dystrophy Association, Chicago, IL, USA.  
14 3. Department of Pediatrics, University of Massachusetts Chan Medical School, Worcester, MA,  
15 USA.  
16 4. Department of Neurology, University of Massachusetts Chan Medical School, Worcester MA,  
17 USA.  
18 5. Horae Gene Therapy Center and The Li Weibo Institute for Rare Diseases Research, University  
19 of Massachusetts Chan Medical School, Worcester, MA, USA.  
20 6. Department of Pathology, Boston Children’s Hospital and Harvard Medical School, Boston,  
21 MA, USA.  
22 7. Department of Clinical Genetics, Institute of Clinical Medicine, University of Tartu, Tartu,  
23 Estonia.  
24 8. Genetics and Personalized Medicine Clinic, Tartu University Hospital, Tartu, Estonia  
25 9. Division of Genetics, Boston Children’s Hospital and Harvard Medical School, Boston, MA,  
26 USA.  
27 10. Department of Cardiology, Boston Children’s Hospital and Harvard Medical School, Boston,  
28 MA, USA.  
29 11. Regulatory Innovation LLC, Raleigh, NC, USA.  
30 12. Charles River Laboratories, Wilmington, MA, USA.  
31 13. Cure Rare Disease, Woodbridge, CT, USA.

32  
33 \* These authors contributed equally to this work.

34 **Corresponding author:** Terence Flotte, email: terry.flotte@umassmed.edu

36 **Summary.** An N-of-1 trial was developed to deliver a dCas9-VP64 transgene designed to  
37 upregulate the cortical dystrophin as a custom therapy for a Duchenne muscular dystrophy (DMD)  
38 patient. After showing signs of mild cardiac dysfunction and pericardial effusion, the patient  
39 acutely decompensated and sustained cardiac arrest six-days after dosing and succumbed two-  
40 days later. Post-mortem examination revealed severe acute-respiratory distress syndrome with  
41 diffuse alveolar damage. Vector biodistribution data was obtained and revealed minimal  
42 expression of transgene in liver. There was no evidence of AAV9 antibodies nor of effector T cell  
43 reactivity. These findings demonstrate innate immune signaling with capillary leak as a form of  
44 toxicity in an advanced DMD case treated with high-dose rAAV gene therapy.  
45

46 **Introduction.** Duchenne muscular dystrophy (DMD) is a fatal, X-linked myopathy caused by  
47 mutations in the dystrophin gene, a large structural gene (2.4 Mb genomic DNA with 79 exons)<sup>1,2</sup>  
48 The large size of the DMD gene predisposes this locus to deletions, duplications and point  
49 mutations<sup>3</sup>. Dystrophin plays a critical role in the function of cardiac myocytes and skeletal  
50 myofibers as part of the dystrophin-glycoprotein complex that anchors myofilaments to the  
51 extracellular matrix and prevents stress-mediated damage to the sarcolemma membrane<sup>4,5</sup>.

52  
53 Several recombinant adeno-associated virus (rAAV)-based approaches to gene therapy for this  
54 disorder have been developed<sup>6-8</sup>. The large size of the dystrophin gene has presented a  
55 challenge for rAAV-based gene replacement, given the 5-kb packaging limit of the vector capsid,  
56 and the need for cis-acting elements, including the AAV inverted terminal repeats (ITRs), a  
57 transcriptional promoter and poly-adenylation signal<sup>9</sup>. This issue has led to several innovative  
58 approaches including mini-dystrophin<sup>10</sup> and micro-dystrophin<sup>11,12</sup> transgenes which include fewer  
59 of the internal rod domain repeats. Another approach to dystrophin correction is to use *in vivo*  
60 gene editing technologies, often based on the CRISPR-Cas9 system<sup>13,14</sup>. RNA-sequence guided  
61 DNA binding can be used to introduce double-strand breaks, as is accomplished with the original  
62 Cas9 nuclease<sup>15</sup>. Alternatively, the property of RNA-guiding DNA binding can direct novel  
63 engineered Cas9 fusion proteins in which the nuclease activity has been inactivated (“dead” Cas9  
64 or dCas9) and transcriptional transactivating domains have been introduced<sup>16-18</sup>. This study  
65 involved such an approach with dCas9 directing the binding of a VP64 transcriptional activation  
66 domain to upregulate a non-muscle full-length isoform of dystrophin (*Dp427c*).

67  
68 Another critical hurdle for rAAV-gene therapy for DMD is the high dose of rAAV that is required to  
69 transduce the extensive mass of tissue that comprises the cardiac and skeletal musculature.  
70 Doses of rAAV used in clinical trials for DMD have ranged from  $5 \times 10^{13}$  to  $2 \times 10^{14}$  vector genomes  
71 per kg body weight<sup>19,20</sup>. Within this dose range, a number of distinct toxicity syndromes have been  
72 observed including hepatotoxicity (often linked to an effector T cell response to capsid or  
73 transgene product), thrombocytopenia and thrombotic microangiopathy (TMA), sometimes  
74 associated with renal toxicity in an atypical hemolytic uremic syndrome (aHUS) picture, and  
75 cardiac toxicity<sup>21</sup>.

76  
77 The case presented here, while tragic in outcome, presents an opportunity to carefully  
78 characterize the systemic, cardiac, and pulmonary toxicities and vector genome biodistribution  
79 more fully in the first week to 10 days after high dose rAAV administration. This case also

80 highlights the increased risk for life threatening severe cardiopulmonary failure in patients with  
81 advanced DMD when they experience complications of early-phase innate immune activation  
82 caused by high-dose rAAV. The short time interval of post-treatment assessments did not allow  
83 sufficient time for significant expression of transgene product in the target organs.

84

85 **Diagnosis and preclinical studies.** The patient was diagnosed with DMD in the first decade of  
86 life and has been on daily steroids (deflazacort at 1.1 mg/kg/day) for over 20 years, with loss of  
87 independent ambulation occurring in his second decade of life. He had progressive decline in his  
88 upper extremity function with increasing cardiopulmonary dysfunction. A skeletal muscle biopsy  
89 revealed patchy dystrophin immunostaining (**Figure 1A**), which was shown to be approximately  
90 3% of control muscle by western blot (**Supplementary Figure S1**). Whole genome sequencing  
91 showed a ~30 kb hemizygous deletion encompassing the promoter and exon 1 of the muscle  
92 isoform (*Dp427m*) of dystrophin inherited from the maternal genome (**Supplementary Figure**  
93 **S2**). Notably, the deletion leaves the promoter and exon 1 of the cortical (*Dp427c*) and purkinje  
94 (*Dp427p*) isoforms of dystrophin intact. We hypothesized that the cortical isoform may be  
95 compensating for the absence of the muscle isoform based on previous reports of exon 1  
96 deletions in *Dp427m* observed in X-linked dilated cardiomyopathy cases that result in no overt  
97 skeletal muscle phenotype<sup>22,23</sup>. RNA-sequencing results from the patient's muscle indeed  
98 detected low transcript expression of dystrophin derived from the cortical promoter (**Figure 1B**).  
99 This finding motivated the design of an individualized therapeutic approach to further upregulate  
100 the full-length *Dp427c* isoform, which differs from *Dp427m* in its promoter and exon 1. Using a  
101 CRISPR activation approach, we identified the optimal sgRNA to target upregulation of *Dp427c*,  
102 first using *in vitro* models, subsequently demonstrating effectiveness in the hDMD/D2-mdx mouse  
103 model harboring a humanized DMD locus (manuscript in preparation). **Figure 1C** shows the  
104 design of the gene therapy construct, which includes the muscle-specific promoter CK8e and  
105 transcription activator VP64 fused to dSaCas9. The size of the transgene insert between the ITRs  
106 is 4558 bp and was successfully packaged into the AAV9 serotype. **Figure 1D** shows the timeline  
107 of the investigational new drug (IND) preparation by Cure Rare Disease (CRD) in collaboration  
108 with Charles River Laboratories, University of Massachusetts Chan Medical School, and Yale  
109 University.

110

111 **Clinical Summary.** The patient (in their 20's) received  $1 \times 10^{-14}$  vg/kg of intravenous CRD-TMH-  
112 001 (IND 28497) consisting of AAV9 vector containing CK8e.dSaCas9.VP64.U6.sgRNA. At that  
113 time, the patient had severe muscle weakness with a low lean muscle mass of 45%, a restrictive

114 pulmonary defect (FEV1=36% predicted; FVC=36%), and mild left ventricular (LV) systolic  
115 dysfunction (LVEF = 54%). He had been on long term steroid treatment (daily deflazacort  
116 equivalent to 1 mg/kg/day of prednisone) for over two decades. Baseline immunologic screening  
117 showed non-detectable AAV9 total antibody (ELISA <1:25, Athena Diagnostics) and negative  
118 ELISPOT responses to AAV9, dSaCas9 (**Figure 2A**). Prophylactic immune suppression therapy  
119 was started 13 days prior to dosing (**Figure 2B**). Safety parameters under study included blood  
120 counts, serum chemistries, brain natriuretic peptide BNP, and troponin I. Treatment emergent  
121 adverse events began 1 day after vector delivery with premature ventricular contractions (PVCs),  
122 followed by a downward trend in platelets (2 days post), and increasing BNP (3 days post) (**Figure**  
123 **2C**). Asymptomatic hypercarbia (pCO<sub>2</sub> 59 mmHg) with respiratory acidosis was noted on safety  
124 monitoring labs 3-4 days post dose. This resolved with optimizing BiPAP pressures from 10/4 to  
125 12/5. Five days post dose the patient developed worsening cardiac function presumed to be  
126 myopericarditis given elevation in troponin and pericardial effusion with tamponade physiology.  
127 The patient developed sudden acute respiratory distress 6 days post dose, with CXR findings of  
128 acute respiratory distress syndrome (ARDS) and worsening cardiac function (EF 45–50%). The  
129 patient progressed to cardiopulmonary arrest and was emergently placed on extracorporeal  
130 membrane oxygenation (ECMO). Despite support with ECMO, the patient passed away 8 days  
131 post-treatment due to multiorgan failure and severe neurological injury. Laboratory studies from  
132 the post-vector period indicated high IL6 (2.8 ng/mL) and a mixed picture of complement  
133 components with elevated C5b-9. Multiplex cytokine bead-based assays revealed elevations of  
134 IL-8 in the serum (**Supplementary Figure S3**) and high levels of IL-6 and MCP-1 in the pericardial  
135 fluid (**Supplementary Figure S4**). Mitigating therapies attempted during this time included  
136 increased steroids, eculizumab (anti-C5), tocilizumab (anti-IL6-R), and anakinra (IL1-R blocker).

137  
138 **Post-mortem Studies.** A consent for limited autopsy allowed for gross and microscopic  
139 examinations of the heart, lungs, brain, triceps, and liver. The post-mortem examination confirmed  
140 markedly decreased muscle mass in the heart and skeletal muscle. Examination of the heart  
141 demonstrated severe cardiomyopathy, characterized by significant gross and histologic fibrofatty  
142 replacement of biventricular myocardium (**Figure 3A**), consistent with what has been described  
143 in dystrophin-deficient cardiomyopathy<sup>24</sup>, and without overt features of active  
144 inflammation/myocarditis, thrombotic microangiopathy, or complement deposition (confirmed by  
145 immunohistochemistry, **Supplementary Figure S5**). The lungs were heavy and edematous (600  
146 gm combined weight, compared with 475 gm expected); the histology showed diffuse alveolar  
147 damage, characterized by hyaline membrane formation along with interstitial and intra-alveolar

148 edema (**Figure 3B**). The findings were in keeping with the clinical impression of ARDS. There  
149 was no evidence of thrombotic microangiopathy or significant inflammation. Gross and  
150 microscopic examinations of the brain demonstrated infarctions in a “watershed” distribution in  
151 the cerebral cortex and cerebellum, and widespread neuronal injury likely reflecting poor perfusion  
152 in the pre-terminal stage (**Supplementary Figure S6**).

153  
154 **Vector Biodistribution.** Analyses of AAV vector DNA distribution were performed using  
155 quantitative real-time PCR (qPCR) (**Figure 3C**). Vector genomes were detected in lung tissue at  
156 a level of 119 vg/diploid genome. Likewise, vector genomes were detected in the myocardium,  
157 with 34 vg/diploid genome in the left ventricle sample and 48 vg/diploid genome in the right  
158 ventricle sample. Vector genome abundance in liver indicated 680 vg/diploid genome. Digital  
159 droplet PCR (ddPCR) was used to confirm vector genome analysis but genome abundance in  
160 liver exceeded upper limit for accurate quantification (**Supplementary Figure S7**).

161  
162 **Expression of Transgene Products.** SaCas9 transcript expression was assessed using qPCR  
163 and revealed no detectable levels in the tissues analyzed except for liver (**Figure 3D**). This pattern  
164 was also observed for SaCas9 protein, as only a faint band was detectable in the liver by western  
165 blot (**Figure 3E**). The absence of the transgene in skeletal and cardiac tissues did not warrant  
166 measurement of *Dp427c* upregulation at this timepoint post-mortem. Expression levels of guide-  
167 RNA showed similar tissue trends (**Supplementary Figure S8**). No AAV9 capsid or Cas9  
168 transgene specific T-cell responses were detected by interferon gamma ELISPOT in patient’s  
169 PBMCs at days 4 or 7 post-dosing (**Figure 2B**).

170  
171 **Discussion and Conclusions.** We present the case of an advanced stage DMD patient who  
172 experienced severe cardiopulmonary toxicity within 6 days following IV administration of rAAV9-  
173 dCas9VP64 at a dose of  $1 \times 10^{14}$  vg/kg. Per our clinic-pathologic findings, we hypothesize this  
174 patient developed a cytokine-mediated capillary leak syndrome, manifested by pericardial  
175 effusion on day 5 and rapidly developing ARDS on day 6. The latter resulted in acute worsening  
176 of pulmonary compliance with respiratory failure, hypoxemia, and an associated acute worsening  
177 of right ventricle heart failure. Unlike other DMD patients in rAAV trials, this patient did not exhibit  
178 evidence of TMA or of adaptive humoral or cell-mediated immune responses to AAV capsid or  
179 transgene products.

180

181 Unfortunately, the acute toxicity and shortened course of this patient prevented a substantive  
182 assessment of the safety and efficacy of the CRISPR-transactivator approach itself. It is well-  
183 known that the single-stranded rAAV genome requires weeks to form transcriptionally active  
184 double-stranded forms after *in vivo* gene therapy. In this case, the innate immune toxicity  
185 shortened the patient's course to an extent that would not have been predicted to allow for  
186 significant transgene expression. While trace amounts of the transgene product were present in  
187 the liver, none was detectable from cardiac or skeletal muscle, and no effector T cell responses  
188 to dCas9 or AAV9 were observed. When comparing vector biodistribution results in our patient  
189 against two patients dosed with systemic administration of Onasemnogene abeparvovec (AAV9)  
190 for Spinal Muscular Atrophy<sup>25</sup>, the vg per diploid genome in the liver are comparable; but notably  
191 higher in the heart, lung, and muscles in our patient; which may be due to the short duration post-  
192 injection. It is plausible that the extensive loss of myofibers in the patient may have altered the  
193 expected vector biodistribution to these tissues. However, this higher vector genome load in our  
194 patient occurred despite dosing at  $1 \times 10^{14}$  vg/kg dose (relative to  $2 \times 10^{14}$  vg/kg for microdystrophin  
195 DMD clinical trials) due to his lower lean muscle mass of 45%. Dose determination will remain a  
196 challenge for custom-designed AAV-mediated therapies, as by definition the precise therapeutic  
197 dose will not have been established.

198  
199 Another recent fatal case was described in a trial involving a non-ambulatory 16-year-old DMD  
200 patient, who passed six days after receiving gene therapy<sup>21</sup>. The patient was part of Pfizer's gene  
201 therapy trial (NCT03362502) and received fordadistrogene movaparvovec at  $2 \times 10^{14}$  vg/kg. His  
202 death is believed to be linked to an innate immune response against the capsid in the  
203 myocardium, which led to cardiogenic shock and heart failure. In our case, we suspected  
204 myocarditis clinically because of an acute rise in serum troponins and pericardial effusion.  
205 However, the opportunity for direct histopathological examination of the myocardial tissue post-  
206 mortem gave definitive evidence of the absence of innate immune cell infiltration typically seen in  
207 myocarditis.

208  
209 There are several novel aspects of our case that add to the body of knowledge relevant to future  
210 applications of AAV-mediated gene therapy to DMD; however, our interpretations and separation  
211 of what is due to the custom gene therapy administered, age of the patient, and severity of disease  
212 state is challenging because of the design of this trial with a unique AAV-mediated gene therapy  
213 for a single patient. The patient's late stage of DMD progression at dosing may have limited his  
214 physiologic reserves to tolerate the cardiopulmonary stress associated with acute toxicity resulting

215 from rAAV gene therapy, but this was not possible to fully demonstrate. Capillary leak syndromes  
216 have been well-described following cytokine release in other gene and cell therapies, including  
217 systemic rAd and CAR-T cell therapies, but not typically after higher doses of AAV for rare genetic  
218 diseases. To our knowledge, this is the first reported case of severe ARDS in AAV gene therapy  
219 in DMD. It is possible that this is unique to the specific product; however, since the toxicity ensued  
220 prior to detectable levels of transgene expression and since the protein composition of the vector  
221 preparations was equivalent to other high-dose AAV9 vectors, it is more likely that this was host-  
222 specific rather than vector-specific. Our interpretation is that the patient described here appears  
223 to have experienced a more severe innate immune reaction than others receiving similar or  
224 slightly higher doses of rAAV in microdystrophin gene therapy trials; thus, further research into  
225 host characteristics predisposing to severe innate immune reactions to AAV may broadly improve  
226 safety of AAV-mediated gene therapy at high doses. As more applications of high-dose IV rAAV  
227 gene therapy are developed the potential for such toxicities should be considered and carefully  
228 monitored among patients whose underlying disease may lessen their ability to tolerate these  
229 adverse effects, especially for custom-designed gene therapy products without prior dosing in  
230 humans.

231

232



233 **METHODS**

234

235 Preclinical assessment was performed on patient quadricep muscle biopsy and dystrophin protein  
236 quantification was performed by western blot and immunostaining. RNA was extracted to perform  
237 RNA-sequencing and assess expression of *DMD* transcripts. Whole genome sequencing was  
238 performed on the patient and mother using blood-derived DNA.

239

240 The patient provided written informed consent for the clinical trial study which was sponsored by  
241 Cure Rare Disease and performed in accordance with protocols approved by the institutional  
242 review board at University of Massachusetts Chan Medical School. Clinical-grade plasmid and  
243 vector were manufactured at Aldevron and Andelyn, respectively. The trial was conducted at  
244 University of Massachusetts Chan Medical School; imaging and safety labs were performed at U  
245 Mass Memorial Hospital Medical center; AAV9 antibody testing was done at Athena Diagnostics.

246

247

248 A limited autopsy was consented by the patient's family in which liver, brain, skeletal muscle,  
249 lungs, heart tissue were evaluated by the pathology department of Boston Children's Hospital.  
250 Postmortem examination was performed 19 hours following death. Macroscopic and microscopic  
251 examination was conducted for each organ. Routine H&E stains were evaluated for  
252 representative sections of each organ. Special stain (Masson trichrome for fibrosis) and  
253 immunohistochemical stains (CD3, CD20 and C4d for T cells, B cells, and complement  
254 deposition, respectively) were performed in selected sections of cardiac tissue. Periodic acid-  
255 Schiff (PAS) stain was performed on selected lung sections to confirm hyaline membrane  
256 deposition. In addition, DNA, RNA and protein were extracted from tissues for vector genome  
257 copy number, transgene transcript and protein quantification, respectively (**Supplementary**  
258 **Method**).

259

260

261

262

263

264

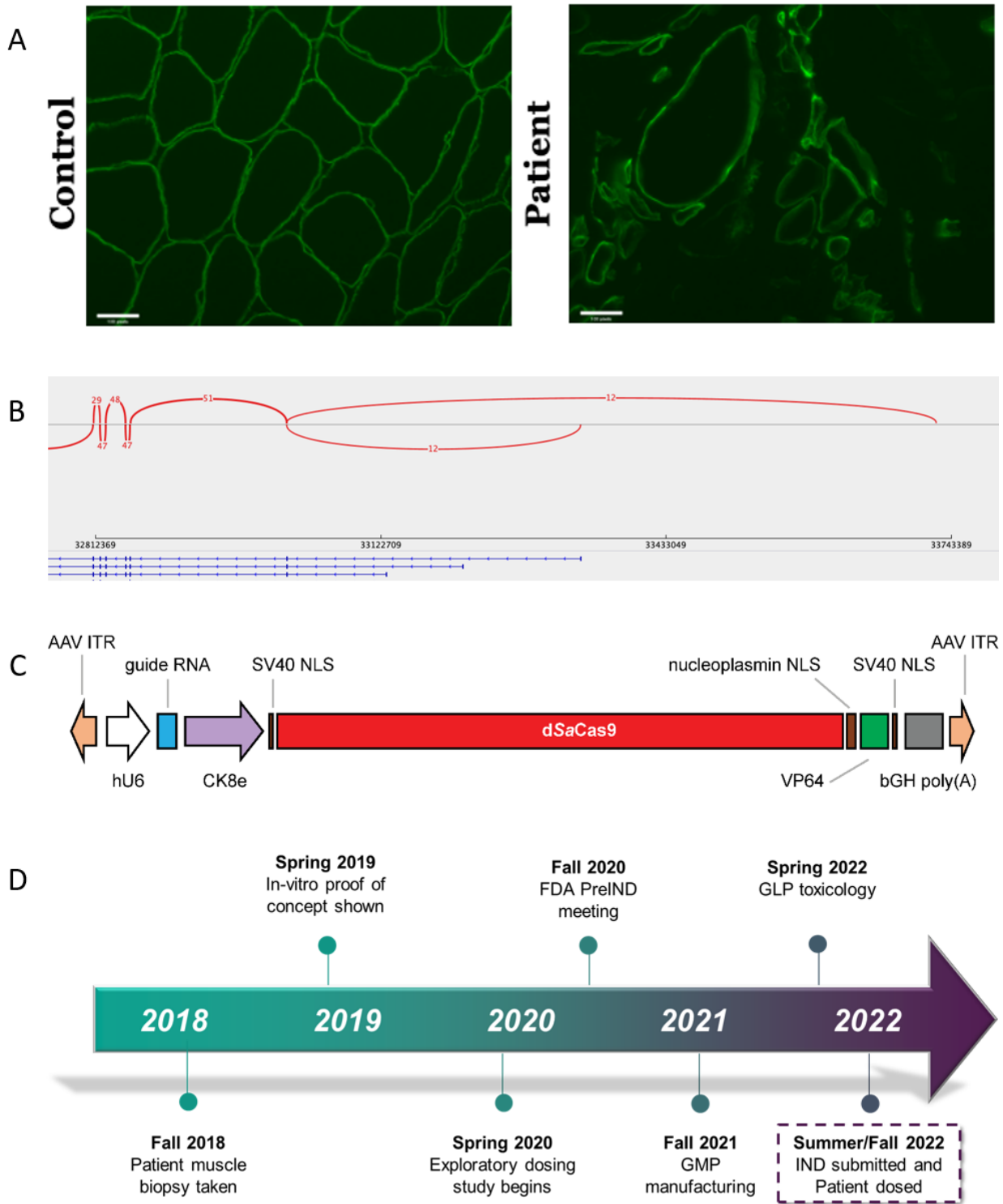
265 **References**

- 266 1. Koenig M, Hoffman EP, Bertelson CJ, Monaco AP, Feener C, Kunkel LM. Complete  
267 cloning of the duchenne muscular dystrophy (DMD) cDNA and preliminary genomic  
268 organization of the DMD gene in normal and affected individuals. *Cell* 1987;50(3):509–17.
- 269 2. Gao QQ, McNally EM. The Dystrophin Complex: Structure, Function, and Implications for  
270 Therapy [Internet]. In: *Comprehensive Physiology*. 2015 [cited 2023 May 8]. p. 1223–  
271 39. Available from: <https://doi.org/10.1002/cphy.c140048>
- 272 3. Duan D, Goemans N, Takeda S, Mercuri E, Aartsma-Rus A. Duchenne muscular  
273 dystrophy. *Nature Reviews Disease Primers* 2021;7(1):13.
- 274 4. Lapidos KA, Kakkar R, McNally EM. The Dystrophin Glycoprotein Complex. *Circulation*  
275 *Research* 2004;94(8):1023–31.
- 276 5. Wilson DGS, Tinker A, Iskratsch T. The role of the dystrophin glycoprotein complex in  
277 muscle cell mechanotransduction. *Communications Biology* 2022;5(1):1022.
- 278 6. Li C, Samulski RJ. Engineering adeno-associated virus vectors for gene therapy. *Nature*  
279 *Reviews Genetics* 2020;21(4):255–72.
- 280 7. Kwon JB, ETTYREDDY AR, VANKARA A, et al. In Vivo Gene Editing of Muscle Stem Cells with  
281 Adeno-Associated Viral Vectors in a Mouse Model of Duchenne Muscular Dystrophy.  
282 *Molecular Therapy - Methods & Clinical Development* 2020;19:320–9.
- 283 8. Manini A, Abati E, Nuredini A, Corti S, Comi GP. Adeno-Associated Virus (AAV)-Mediated  
284 Gene Therapy for Duchenne Muscular Dystrophy: The Issue of Transgene Persistence.  
285 *Frontiers in Neurology* [Internet] 2022;12. Available from:  
286 <https://www.frontiersin.org/articles/10.3389/fneur.2021.814174>
- 287 9. Wu Z, Yang H, Colosi P. Effect of Genome Size on AAV Vector Packaging. *Molecular*  
288 *Therapy* 2010;18(1):80–6.
- 289 10. Zhang Y, Duan D. Novel Mini-Dystrophin Gene Dual Adeno-Associated Virus Vectors  
290 Restore Neuronal Nitric Oxide Synthase Expression at the Sarcolemma. *Human Gene*  
291 *Therapy* 2012;23(1):98–103.
- 292 11. Davies KE, Guiraud S. Micro-dystrophin Genes Bring Hope of an Effective Therapy for  
293 Duchenne Muscular Dystrophy. *Molecular Therapy* 2019;27(3):486–8.
- 294 12. Duan D. Micro-Dystrophin Gene Therapy Goes Systemic in Duchenne Muscular Dystrophy  
295 Patients. *Human Gene Therapy* 2018;29(7):733–6.
- 296 13. Happi Mbakam C, Rousseau J, Tremblay G, Yameogo P, Tremblay JP. Prime Editing  
297 Permits the Introduction of Specific Mutations in the Gene Responsible for Duchenne  
298 Muscular Dystrophy. *International Journal of Molecular Sciences* 2022;23(11).
- 299 14. Chemello F, Chai AC, Li H, et al. Precise correction of Duchenne muscular dystrophy exon  
300 deletion mutations by base and prime editing. *Science Advances* 7(18):eabg4910.

- 301 15. Jinek M, Chylinski K, Fonfara I, Hauer M, Doudna JA, Charpentier E. A Programmable  
302 Dual-RNA–Guided DNA Endonuclease in Adaptive Bacterial Immunity. *Science*  
303 2012;337(6096):816–21.
- 304 16. Qi LS, Larson MH, Gilbert LA, et al. Repurposing CRISPR as an RNA-Guided Platform for  
305 Sequence-Specific Control of Gene Expression. *Cell* 2013;152(5):1173–83.
- 306 17. Mali P, Aach J, Stranges PB, et al. CAS9 transcriptional activators for target specificity  
307 screening and paired nickases for cooperative genome engineering. *Nature Biotechnology*  
308 2013;31(9):833–8.
- 309 18. Lek A, Ma K, Woodman KG, Lek M. Nuclease-Deficient Clustered Regularly Interspaced  
310 Short Palindromic Repeat-Based Approaches for In Vitro and In Vivo Gene Activation.  
311 *Human Gene Therapy* 2021;32(5–6):260–74.
- 312 19. Duan D. Systemic AAV Micro-dystrophin Gene Therapy for Duchenne Muscular  
313 Dystrophy. *Molecular Therapy* 2018;26(10):2337–56.
- 314 20. Elangkovan N, Dickson G. Gene Therapy for Duchenne Muscular Dystrophy. *Journal of*  
315 *Neuromuscular Diseases* 2021;8(s2):S303–16.
- 316 21. Lek A, Atas E, Hesterlee SE, Byrne BJ, Bönnemann CG. Meeting Report: 2022 Muscular  
317 Dystrophy Association Summit on ‘Safety and Challenges in Gene Transfer Therapy.’  
318 *Journal of Neuromuscular Diseases* 2023;10(3):327–36.
- 319 22. Ferlini A, Sewry C, Melis MA, Mateddu A, Muntoni F. X-linked dilated cardiomyopathy and  
320 the dystrophin gene. *Neuromuscular Disorders* 1999;9(5):339–46.
- 321 23. N Cohen, F Muntoni. Multiple pathogenetic mechanisms in X linked dilated  
322 cardiomyopathy. *Heart* 2004;90(8):835.
- 323 24. Kamdar F, Garry DJ. Dystrophin-Deficient Cardiomyopathy. *Journal of the American*  
324 *College of Cardiology* 2016;67(21):2533–46.
- 325 25. Thomsen G, Burghes AHM, Hsieh C, et al. Biodistribution of onasemnogene abeparvovec  
326 DNA, mRNA and SMN protein in human tissue. *Nature Medicine* 2021;27(10):1701–11.

327  
328  
329  
330  
331  
332  
333  
334  
335  
336  
337  
338  
339  
340

341 **FIGURE 1: Preclinical assessment and planning towards IND.**



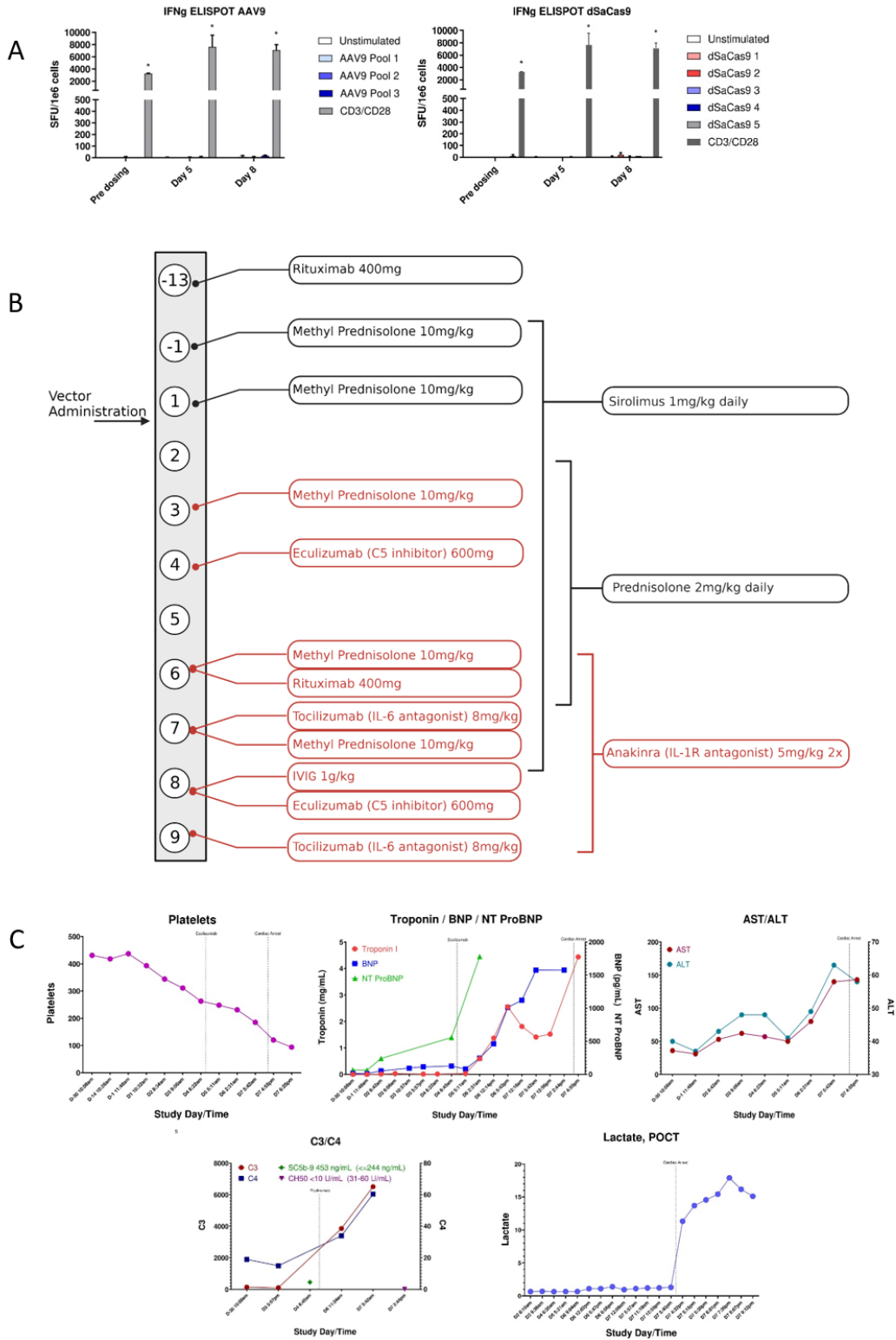
342

343 **A)** Frozen muscle tissue section from a de-identified unaffected individual (left) and the proband

344 (right) immunostained for dystrophin. Dystrophin staining is visible at the myofiber sarcolemma in

345 the unaffected control sample and also in several myofibers of different sizes in the proband. The  
346 positive staining was detected using antibodies to the dystrophin rod domain and C-terminus  
347 (CAP 6-10 antibody generated in Kunkel Lab). **B)** Bottom panel: RNA sequencing reads showing  
348 exons 1–6 (right to left) of the full length *Dp427c* (cortical), *Dp427m* (muscle), and *Dp427p*  
349 (Purkinje) DMD isoforms (from top to bottom). Top panel: number of reads that span exons (arcs).  
350 Only the DMD cortical isoform is expressed in patient muscle as indicated by reads from *Dp427c*  
351 exon 1. **C)** The therapeutic construct was cloned into a plasmid backbone with AAV2 ITRs  
352 (Addgene #99680). The guide RNA expression is regulated by a human U6 promoter and the  
353 expression of the dSaCas9-VP64 fusion protein is regulated by a CK8e promoter (Hauscka Lab,  
354 University of Washington), which was engineered from the regulatory elements from mouse  
355 muscle-type creatine kinase. dSaCas9, dead *Staphylococcus aureus* Cas9. NLS (nuclear  
356 localization sequence), bGH poly(A), (bovine growth hormone polyadenylation signal). **D)** Patient  
357 muscle biopsy was performed at University of Massachusetts Chan Medical School in Fall 2018.  
358 *In vitro* proof of biology was completed in Spring 2019. Exploratory pharmacology studies  
359 performed in collaboration with CRL during Spring 2020. The pre-IND meeting with Food and  
360 Drug Administration (FDA) occurred in Fall 2020 and good manufacturing practice (GMP) AAV  
361 manufacturing was performed by Andelyn (**Supplementary Table S1**) in Fall 2021 and then good  
362 laboratory practice (GLP) toxicology studies commenced in Spring 2022. This culminated in the  
363 IND submission in Summer 2022 and patient dosing thereafter.  
364

365 **FIGURE 2: Clinical trial data.**



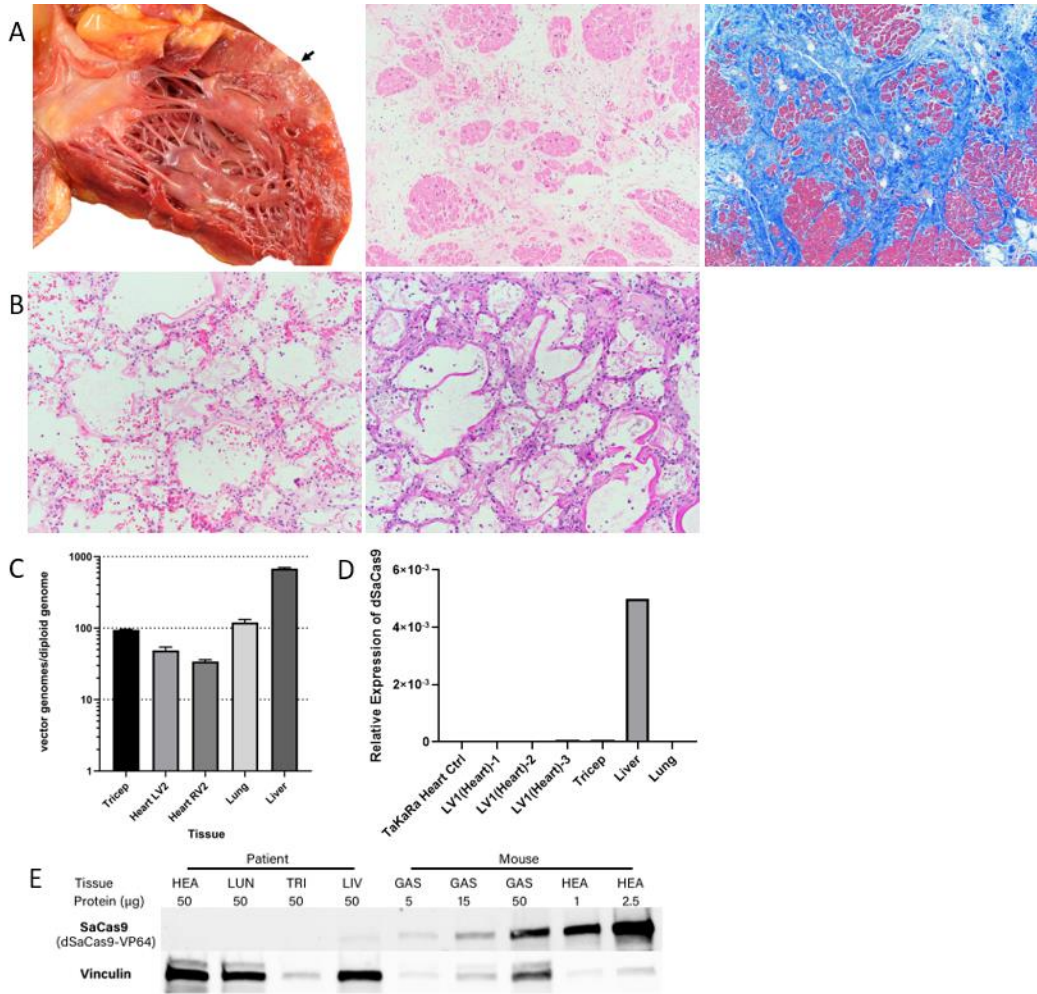
366

367

368 **A)** Interferon-gamma ELISPOT assays for AAV9 and SaCas9 in patient samples. PBMCs isolated  
369 from the patient at different time-points in life were stimulated by either AAV9 (left) or dSaCas9  
370 (right) peptide pools to assess T-cell responses by interferon- $\gamma$  ELISPOT assay. Negative controls  
371 were unstimulated cells, and CD3/CD28 stimulation was used as positive control. Data was run  
372 in technical triplicates and reported as mean  $\pm$ SD. Significance designated by \* represents 3x  
373 negative control. Peripheral blood mononuclear cells (PBMCs), spot forming unit (SFU) standard  
374 deviation (SD). **B)** Timeline of prophylactic immune suppression administered during clinical trial.  
375 Numbered circles denote day of treatment - beginning 13 days pre-treatment to 9 days post-  
376 treatment. Drugs shown in black text were listed on the clinical trial protocol, drugs shown in red  
377 were not. **C)** Monitoring of cardiac, complement and liver markers during clinical trial period  
378 (beginning 30 days prior to vector administration).

379

380 **FIGURE 3 Post-mortem analysis of patient tissues.**  
 381



382 **A)** Macroscopic examination of the heart demonstrates fibrofatty replacement of the left  
 383 ventricular wall (arrow); histologic evaluation of this area shows marked interstitial fibrosis and  
 384 fatty replacement with residual cardiac myocytes; there is no histologic evidence of myocarditis  
 385 or thrombotic microangiopathy (H&E and Masson trichrome stains, 4X). The findings are in  
 386 keeping with severe cardiomyopathy. **B)** Microscopic examination of the lungs shows diffuse  
 387 alveolar damage, characterized by hyaline membrane deposition with interstitial and intra-alveolar  
 388 edema (H&E and PAS stain, 10X). **C)** Vector biodistribution in patient tissues. Vector genomes  
 389 were quantified by qPCR and calculated to indicate vector genomes per diploid genome for each  
 390 tissue. Data was run in technical triplicates and reported as mean ±SD. Quantitative polymerase  
 391 chain reaction (qPCR) standard deviation (SD). **D)** RNA expression levels of dSaCas9 were  
 392 measured by RT-qPCR. Heart tissue was sampled in three different locations. **E)** SaCas9  
 393 expression in post-mortem tissue compared to AAV-injected mice at similar dosage. Protein  
 394  
 395



396 expression in GAS and HEA mouse tissue is from 8-week time point compared to 8-day post-  
397 treatment from patient tissues. Vinculin was used as a loading control but showed variable relative  
398 expression in non-muscle tissues. HEA, heart; LUN, lung; TRI, triceps; LIV, liver; GAS,  
399 gastrocnemius.

400

401

402

403

404

405

406

407